The Consolidated Mathews Stability Graph for Open Stope Design

Ali Mortazavi (ali.mortazavi@nu.edu.kz)
Nazarbayev University
Bakytzhan Osserbay
Nazarbayev University

Research Article

Keywords: Underground mining, Mathews Stability Graph, Open stope design

Posted Date: July 6th, 2021

DOI: https://doi.org/10.21203/rs.3.rs-191163/v1

Version of Record: A version of this preprint was published at Geotechnical and Geological Engineering on January 16th, 2022. See the published version at https://doi.org/10.1007/s10706-021-02034-0.

The Consolidated Mathews Stability Graph for Open Stope Design

Ali Mortazavi*, Bakytzhan Osserbay

School of Mining & Geosciences, Nazarbayev University, 53 Kabanbay Batyr Ave., Nur-Sultan, 010000, Kazakhstan, Tel.:+7-705-440-3066; E-mail: ali.mortazavi@nu.edu.kz
*Corresponding Author: Ali Mortazavi

ABSTRACT

The stability graph method of stope design is one of the most widely used methods of stability assessments of stopes in underground polymetallic mines. The primary objective of this work is to introduce a new stability chart, which includes all relevant case histories, and to exclude parameters with uncertainties in the determination of stability number. The modified stability number was used to achieve this goal, and the Extended Mathews database was recalculated and compared with the new stability graph. In this study, a new refined Consolidated stability graph was developed by excluding the entry mining methods data from the Extended graph data, and only the non-entry methods data was used. The applicability of the proposed Consolidated stability chart was demonstrated by an open stope example. The stability for each stope surface was evaluated by a probabilistic approach employing a logistic regression model and the developed Consolidated stability chart. Comparing the stability analysis results with that of other published works of the same example shows that the determined Consolidated chart, in which the entry-method data is excluded, produces a more conservative and safer design. In conclusion, the size and quality of the dataset dictate the reliability of this approach.

Keywords: Underground mining, Mathews Stability Graph, Open stope design

LIST OF SYMBOLS AND ABBREVIATIONS

A: Rock stress factor
B: Joint orientation adjustment factor
C: Gravity adjustment factor
CDF: Cumulative distribution function
ELOS: Equivalent Linear Overbreak/Slough
F: Fault factor
HR: Hydraulic radius (in meters)
J_a : Joint alteration number
J_n : Joint set number
J_r : Joint roughness number
J_w : Joint water reduction factor
JKMRC: Julius Kruttschnitt Mineral Research Centre
K: Stress ratio ($\sigma_H : \sigma_V$)

N: Mathews stability number
N': Modified stability number
NGI: Norwegian Geotechnical Institute
P: Predicted logit value
Q: Tunnelling Quality Index
Q': Modified Q value
RF: Radius Factor
RMR: Rock Mass Rating (Bieniawski)
S: Shape factor
SRF: Stress Reduction Factor
$X_1 \ldots X_k$: Logit model dependent X variables
Z: Predicted log odds value
a: Regression parameter without dependent X variable. A constant in the logit regression equation.
ƒ(z): Predicted logit probability value

1. Introduction

The Mathews stability graph is an empirical model that predicts the stability of open stope surfaces and has been extended to predict the onset of continuous caving. The stability graph was developed based on the commonly used rock mass classification systems, the Q-system proposed by Barton et al. (1974) and the RMR proposed by Bienawski (1973) (Potvin 1988). These rock mass classification systems provided the framework to develop mine geotechnical models as appropriate to underground mine design. The stability graph method of stope design has been modified since it was introduced and has been used as a design method within the mining industry worldwide. The initial database used in the development of the method consisted of 26 case histories from three mines in Canada. Potvin (1988), modified the database used in the method by increasing the number of case studies to 176. Trueman and Mawdesley (2003) used the initial factors and enhanced the database by increasing the number of case histories to 487, including about 75 case histories from Potvin. After the development of the stability graph, this stability analysis method has gone through several modifications and improvements and it is difficult to choose the appropriate approach because these graphs are based on different methods of calculating stability number. In order to enhance the accuracy and consistency of the stability graph, new factors such as fault factor, the effects of induced tensile stresses, opening stand-up time, and 3D stress state have been considered. These efforts have not been systematically incorporated into the method and often making it more challenging to use the stability charts. This work aims to propose a new alternative stability graph which is based on the modified stability number introduced by Potvin (1988), recalculates the more extensive database of the Extended Mathews stability graph, incorporates all relevant case histories into on single stability chart and all relevant modifications to the stability number and eliminating entry mining methods form the database.

2. Background

As a design tool for stope stability assessments, Mathews' stability graph approach has acquired worldwide recognition (Potvin and Hadijegeorgiou 2001) as illustrated in Fig. 1. This approach has been applied in countries such as Canada, Australia, Europe, Africa, Chili, and the United States (Vallejos et al. 2018). Mathew's stability graph was initially developed for open stopes where depths were greater than 1000 meters (Mathews et al. 1981).

Trueman et al. (2000) stated that the majority of case studies of the original report come from the mining depths which are greater than 1000 meters, and the original database included 26 cases.

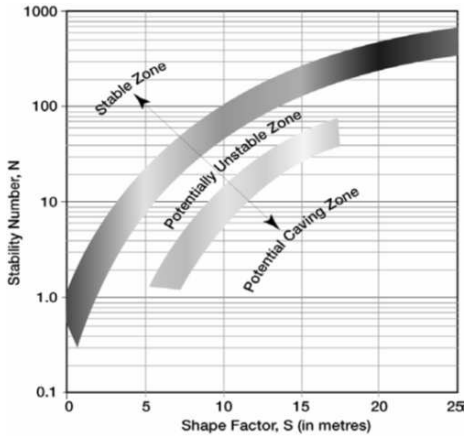

Fig 1 The Mathews Stability Graph (Mathews et al. 1981)

Mathews et al. (1981) suggested that rock mass classification systems could be applied for open stope design. Mawdesley et al. (2001) included the existing empirical relationships between rock mass in-situ properties and joint orientation, induced stress, and stope surface dimensions into the method. In the original stability graph, the hydraulic radius was used as the measure of stope surface geometry (Mathews et al. 1981). Hydraulic radius was proposed in the work of Laubscher and Taylor (1976), and it is expressed as the ratio of the stope surface area to the stope surface perimeter. Mathews et al. (1981) proposed stability number (N) which consists of geotechnical factors such as A, B, C, and Q', and the stability number can be calculated using Equation (1) where Q represents the rock mass quality index in Barton's rock mass classification system (Barton et al. 1974) considering that the joint water reduction factor and SRF are 1. Additionally, A, B, and C are the stress, joint orientation, and gravity factors.

$$N = Q \times A \times B \times C \qquad (1)$$

The stress factor A is derived from the ratio of intact rock UCS (σ_c) to the induced compressive stress (σ_I) acting on the plane of the stope face (Stewart, 2005). The magnitude of induced stresses can be determined by numerical modelling (Mathews et al., 1981). The rock stress factor varies between 0.1 to 1.0, and it is linearly related to σ_c/σ_I (Stewart, 2005). Factor B takes into account the location of the most critical structure with respect to the stope surface. Joint sets, foliation planes, or bedding planes are examples of critical structures (Potvin and Hadjigeorgiou 2001). The assumption that the effect of gravity force acting on horizontal surface stability is eight times higher than its action on a vertical surface is used as a basis in the definition of the gravity adjustment factor, C. The gravity adjustment factor considers the effects of gravity on stope surface stability due to slabbing, falling, and sliding (Mathews et al., 1981). The relationship between the gravity adjustment factor, C, and the dip angle of the surface is given as below:

$$Factor\ C = 8 - 7 \times Cos\ (Angle\ of\ Dip) \qquad (2)$$

2.1. The Modified stability graph

To develop a revised stability graph, new cases were collected, and the number of cases was increased to 176 in the period between 1986 and 1987 (Potvin 1988). The new modified stability chart is illustrated in Fig. 2. The application of the Modified stability graph led to an increase in its applicability since the quantity and quality of the dataset dictates the confidence of the stability chart. However, Trueman and Mawdesley (2003) reported that in approximately 100 case histories there were uncertainties in data.

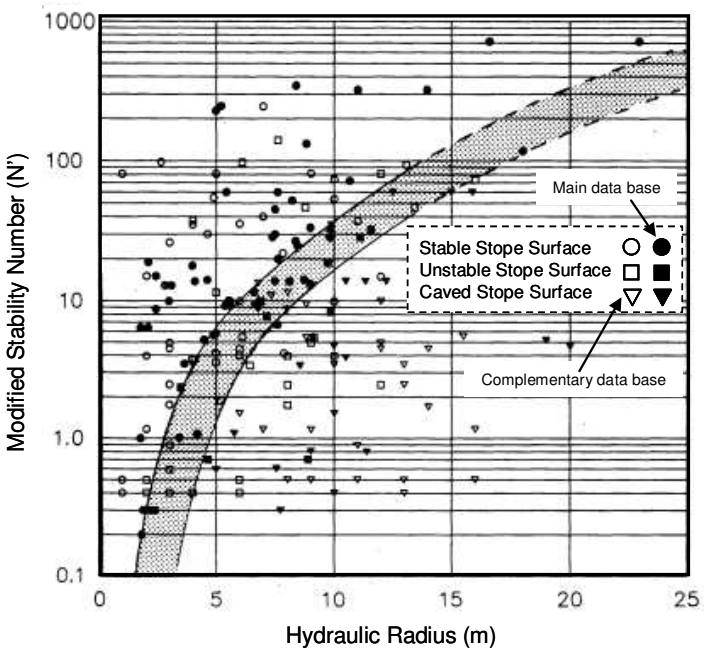

Fig 2 The Modified Stability Chart (Potvin 1988)

2.2. Extended Mathews stability graph

The Extended Mathews stability graph was proposed by Trueman et al. (2000) and Mawdesley et al. (2001). In these investigations, the number of case studies was increased from 176 to 485. In this version of the stability graph, the 100 cases which were earlier noted in the modified stability graph, where uncertainties were present, were removed from the new database. The originally proposed Mathews et al. (1981) method of calculating the stability number was used for all case studies. The additional cases included more significantly larger stopes and a more extensive range of stability numbers (Stewart, 2005). The Extended Mathews stability chart is based on the initial framework of the method which is based on stability number (N) and hydraulic radius and includes only two stability boundaries. Mawdesley (2002) used logistical analysis and determined that there were no considerable differences between failure and major failure, thus the boundary of failure-major failure could not be justified (Stewart 2005). Moreover, in the work of Potvin (1988) the stress factor A is taken as 0.1 where the ratio of intact rock UCS (σ_c) to the induced stress (σ_I) is less than two. In the works of Trueman et al. (2000) and Mawdesley et al. (2001), the stress factor A

proposed by Potvin (1988), was used. Furthermore, the use of logistic regression in the work of Mawdesley et al. (2001) enabled the definition of the boundary between failed and stable stopes statistically.

According to Trueman et al. (2000) and Mawdesley (2002), an accurate delineation of the boundaries was carried out and the significance of the boundaries was carefully checked by an increase in the range of data to determine the boundaries of the Extended Mathews Stability graph. Also, the advantageous side of the Extended Mathews stability graph, in comparison with other stability graphs, is that this approach includes the largest database including complex stope geometries (Stewart 2005).

2.3. Formulations of Stability Chart Parameters

Mathews et al. (1981) proposed the stability number as given in Equation (1). Increasing the number of case studies, the formulation of factors A, B, and C was revised by Potvin (1988), and led to the formulation of the modified stability number N'. Suorineni (1998) stated that the accumulated experience in using factors A, B, and C shows that the stress and gravity factors still need to be redefined. Moreover, to take into account the effects of nearby fault/shear zones a fault factor parameter needed to be used. Given that the original formulation was easier to calculate with fewer factors, the original method of determining N was used in the Extended Mathews method. However, the modified method of determining N has been more common among mining industry practitioners. In this work, all input data is consolidated employing the modified stability number.

In the original Mathews' stability graph as well as the modified stability graph, the definition of the hydraulic radius (HR) is implemented to determine the shape factor. According to Milne et al. (1996) and Potvin and Hadjigeorgiou (2001), when the hydraulic radius is applied for irregular geometry, it has essential limitations, even though this parameter demonstrated its value when considering the size and shape of an excavation (Stewart and Trueman 2001). Milne et al. (1996) stated that for irregular geometries the usage of radius factor (RF) for estimating the distance to the supports gives a more rigorous result. To calculate the radius factor, Equation (3) is used, where r_θ is the distance between supports and surface center.

$$RF = \frac{HR}{2} = \frac{0.5}{\frac{1}{n}\sum_{\theta=1}^{n}\frac{1}{r_\theta}} \quad (3)$$

As illustrated in Fig. 3, Milne et al. (1996) compared the hydraulic radius versus radius factor for a rectangular body with an increasing 100 meters of length. As can be seen from Fig. 3, the hydraulic radius is more sensitive, while the radius factor is less when is related to the range which outstrips the width about four times. According to Hoek et al. (1995), the supporting effect of the tunnel face is insignificant at about 1.5 times the tunnel span. Accordingly, Milne et al. (1996) suggested that the use of the radius factor leads to a more realistic assessment of the effect of two-way spanning compared to the hydraulic radius. In the work of Milne et al. (1996) three case histories were presented where the use of radius factor in the back-analyses, enhanced the reliability of initial stability assessments which were based on the hydraulic radius.

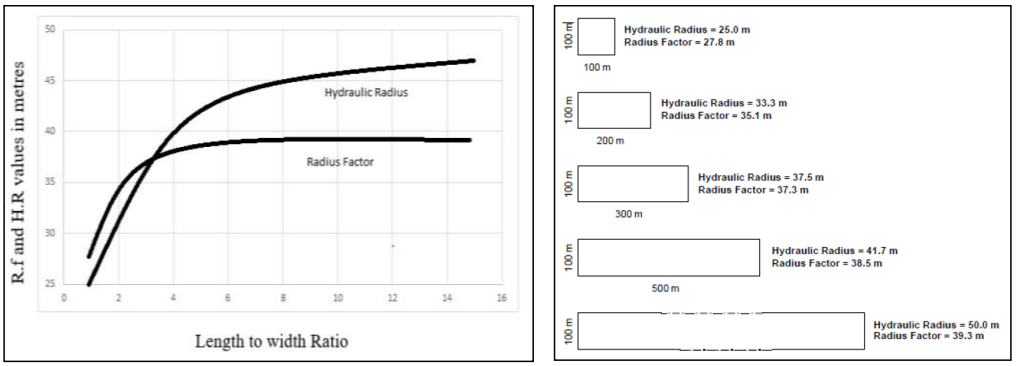

Fig 3 A Comparison of variations of radius factor and hydraulic radius (Milne et al. 1996)

The background for the development of the fault factor is that faults that are near to stope walls impact the tensile stress distribution, thus increasing overbreak and dilution. In the study of Clark and Pakalnis (1997), seven generic fault factor curves, which are related to Equivalent Linear Overbreak/Slough (ELOS) contours, were proposed. Concerning the significance of dilution in mining, they presented a new stability graph to enable the evaluation of dilution. It should be realized that only 85 case studies were used in the development of these charts which, may be insufficient to define stability zones confidently (Clark and Pakalnis 1997). The objective was to use various cavity monitoring systems to determine 3D stope geometry. ELOS values and logistic regression with engineering judgment were utilized to determine ELOS dilution chart zones. Furthermore, to evaluate fault factor, Suorineni et al. (2001) proposed a methodology that takes into consideration the following factors:

- The stope surface and fault angle
- Fault shear strength
- The aspect ratio of stope
- The fault distance from stope and stope dip
- In-situ stress ratio (k)

In the original stability graph, the open stope stability is evaluated according to three design sectors: stable, unstable, and cave. These zones were divided by ‘‘eyeballing’’ based on the cluster of points that indicated the stability state cases. The original Mathews stability graph evaluated the stability states by three different zones while Potvin “eyeballed” the data points into stable and failed cases using a single boundary. Stewart and Forsyth (1995) criticized Potvin’s approach because engineers can mistakenly assume that stopes are either stable or cave. They proposed three boundaries that will divide the stability graph into four zones of stable, potentially unstable, potential major failure, and potential caving as illustrated in Fig. 4. Concerning the empirical nature of presented stability graphs, they enable an approximate prediction of stope behavior and do not provide accurate stability analysis. Mawdesley et al. (2001) extended the database of Mathew’s stability graph to 485 aiming at increasing its reliability. According to Trueman and Mawdesley (2003), this improvement in the database led to the change of boundaries of the extended stability graph.

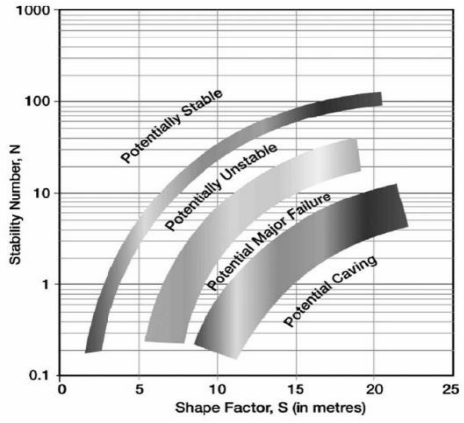

Fig 4 The stability graph boundaries (Stewart & Forsyth 1995)

3. Development of a Consolidated Mathews Stability Graph

3.1. Application of Statistical Methods to Stability Graph

With regard to the development history of the stability zones on the Mathews stability chart, the nature and placement of boundaries of stability zones were changed as appropriate to the newly-added data. Determining the position of stability zones on the stability graph is essential, and as it is conducted visually, it affects the reliability of the method (Mathews et al. 1981; Potvin 1988). Nevertheless, a numerical calculation of stability zone position and width is a way of enhancing the reliability of Mathew's method (Mawdesley 2002).

Potvin (1988) was the first author who proposed the use of statistics in determining the position of stability boundaries, but Nickson (1992) was the one who took the first steps toward it and tried to define the position of stability boundaries through statistics. Nickson (1992) attempted to distinguish between caving and stable cases and determined the associated support boundaries on the modified stability graph. To conduct this, he introduced Mahalanobis distance and discriminant analysis to the stability database and, the logarithmic transformation was used to obtain a linear separation between the caved and unsupported stable cases. In this analysis, unstable cases were not investigated, and separation line for caving and unstable zones or unstable and stable zones were not determined. Furthermore, the stable-caved boundary determined by Nickson was compared against Potvin's transition zone. Based on obtained results, Nickson advised that the transition zone developed by Potvin can be utilized for unsupported stope surface design. Furthermore, statistical approaches utilized throughout the years were Mahalanobis distance, the Bayesian likelihood discrimination method, and the logistic regression method (Mawdesley 2002).

Liao (1994) stated in his work that the discrete nature of the dependent variable is not reflected in an ordinary linear regression, and to avoid problems with binary outcomes, the logistic regression should be used. The application of logistic regression depends on the data and the logit model was selected in this work. The logit model uses a non-linear transform of the true/false (0 and 1) probability scale. The estimated probability of the true option occurs by using the logit function for the combination of independent variables. Mawdesley (2002) defined intermediate categories of stability estimates by changing the probability scale over zero to one.

In the proposed approach in this paper, the stability number (N) and the shape factor (S) were considered as two independent variables and observed in each stability dataset. In the logistic regression, the data which fits a maximum likelihood model is binary and the predicted probability values can be obtained by curve fitting. The predicted logit values differ from the dependent variable values, and the dataset does not perfectly match with the logit function. In the logit model, the predicted outcomes can be compared with original data to minimize inconsistency cases. The values of stable outcomes that lie in the failure zone can be classified as incompatibles and the orientation and proportion of incompatible points can be altered when changing stability boundaries.

The predicted logit value is the predicted values of the dependent variable which are obtained from the logit model (Mawdesley 2002). In the work of Mawdesley (2002), by implementing the maximum likelihood method, the unknown parameters α, β_1, β_2 … β_k is estimated as below. To find the predicted risk the estimated values of α, β_1, β_2 … β_k are used and the equation for the logit function is given in the following form:

$$Z = \alpha + \beta_1 X_1 + \beta_2 X_2 + \beta_3 X_3 \dots\dots + \beta_k X_k = \alpha + \sum \beta_k X_k \quad (4)$$

$$P = \frac{1}{(1+e^{-Z})} \quad (5)$$

Where,

Z: the predicted logit value

P: the predicted logit probability value

α: regression parameter (a constant)

$\beta_{1,2\dots k}$: regression coefficients, and

$X_{1,2\dots k}$: independent variables

3.2. Stope design database development

With regard to the published literature, it is realized that the stability graph is introduced for open stope design at depths below 1000 meters. The stability graph has gone through several modifications (e.g. extending the number of case histories, implementing new factors such as fault factor or time, etc.) since it was introduced initially. The method has been used extensively worldwide and it is a reasonably accurate empirical design approach. In this work, the database of the Extended Mathews stability was recalculated, and as a basis, the modified stability number was implemented, and a new stability graph was proposed. In this study, all entry mining methods data were removed from the Extended stability chart database and non-entry mining methods were the focus of the study. Accordingly, the relevant data including case studies were compiled in the form of a Consolidated Mathews stability graph.

The data used in this work was taken from the Extended Mathews database which consists of case histories from works of various authors (Mathews et al. 1981; Potvin 1988; Nickson 1992; Mawdesley 2002) and also the data from

Julius Kruttschnitt Mineral Research Centre (JKMRC), which was compiled from numerous investigations and field surveys. The data were read into the Microsoft Excel statistical analysis environment and a comprehensive analysis was carried out. The database was revised and recalculated several times to find the errors in the data. With regard to the objectives of the study, all entry mining methods data were eliminated and only non-entry mining methods were considered. Hence, the number of case histories was reduced from 485 to 244 aiming at developing a new empirical design chart for non-entry mining methods. For the Extended stability graph, the stability number remained the same while for the Consolidated stability graph the stability number (N) of Extended Mathews database was recalculated based on adjustment factors of Potvin's Modified stability graph (1988). The logistic regression was used to determine the stability zone boundaries. To construct the Consolidated stability graph, the XLSTAT software was implemented to perform logistic regression as a primary tool in this work. XLSTAT is an extension pack of Microsoft Excel which allows performing statistical analysis, prediction analysis, and regression analysis.

3.3. Statistical analysis and application of the logit model to the development of stability graph

Logistic regression is a method that enables the statistical analysis of a dataset, in which there are independent variables, and determines an outcome. The outcome of the method is expressed by a dichotomous variable in which there are only two possible outcomes and has the capability to estimates the proportion of each outcome. Application of this method enables the calculation of the probability of the stability of a stope of a given geometry. In this study, a logistic regression analysis was conducted. In the traditional regression techniques and ordinary linear regression, it is difficult to demonstrate the interval nature of the dependent variable.

To construct the logit model for 224 cases, three parameters were taken as inputs; Mathews stability number (N), the shape factor (S), and the stability outcome. In the logit model, the probability range for a stable outcome was denoted as one while for failure outcome it was defined as zero and degrees of instability in between. To analyze the accuracy and validity of the model and the variable nature of the data, the obtained logit probability values were compared against actual observed stability cases. To redefine the three classes of stability (stable, failure, major-failure), the stability data of the Mathews was investigated by implementing a three-level logit model. In the logit model, the outcomes are generally yes/no results but to model the three stability classes two transitional categories were implemented, to analyze the stability database. Between the classes of stability, the two separation lines were produced by the logit model, and the function of the logit model is such that the separation lines are parallel. To determine stability zones boundaries, the binary model was used and the results were compared against the three-level logit model, which was substantiated as an acceptable assumption.

The next step was to determine the actual position of the boundaries. To find the best location and outline for the stability zones and propose an estimation of probabilities for each category based on the data conditions, it was necessary to count the numbers of each category of stability in thin stripes in the form of parallel lines of separation. In the model, an optimal range of cumulative logit values was used to define each class of stability with the usage of bands by logistic regression. To define the best outcome for cumulative distribution and probability function in terms of smoothness and resolution, various range of bin sizes were probed. The percentage of a given stability class in each bin was calculated and accumulated to determine the Cumulative Distribution Function (CDF) of each stability class. To determine the optimal placement of stability boundaries, the inverse curve was plotted, as assistance, for each class of stability (see Fig. 5). On the CDF graph, the logits probability values are determined by the intersection points.

Experience with this data set has shown that the use of a logarithmic transform in the logit model, which gives rise to the terms *ln N* and *ln S*, is better due to the extended range of the data and because the logarithmic transforms give a linear separation for the stability classes (Mawdesley, 2002). Accordingly, to determine the stability zones Equation (4) was used and the values for the corresponding α, β_1, and β_2 were obtained from the logistic regression model as 3.146, -1.173, and 0.8409 respectively.

$$Z = 3.146 - 1.173 \ln S + 0.8409 \ln N \quad (6)$$

Where

Z: the predicted log value,

S: the shape factor, and

N: the stability number

To estimate the predicted log value, Equation (5) was rearranged as Equation (7), and predicted log values are calculated from:

$$Z = \ln \left(\frac{p}{1-p}\right) \quad (7)$$

Where,

Z: the predicted log value, and

P: the predicted logit probability value determined from the CDF graph

The boundaries for the graphs are mathematically expressed in the following form. The advantages of a mathematical description of boundaries, as opposed to boundary delineation by eye, is the improved objectivity and ability in the quantification of the variance of the stable-failure boundary.

$$N = e^{\frac{(z-\alpha-\beta 1 lnS)}{\beta_2}} \quad (8)$$

Where

N: the Mathews stability number

S: the shape factor

α: regression parameter, and

β_1 and β_2: regression coefficients

The primary purpose of the use of the CDF plot is to define intersection points. In Fig. 5 the stable class curve intersects with the inverse failure class curve and presents a stable-failure intersection point. The failure-major

failure cross over point is located where the failure curve intersects with the inverse major failure curve on the CDF plot. Due to the irregularity of the major failure cumulative distribution curve, a straight line was fitted to the curve visually and was used as a guide to determine the failure-major failure cross-over (Fig. 5). The CDF of stable classes (stable, failure, and major failure) represents part of data below the stability boundary which is denoted by a known logit value, while the inverse CDF indicates the part of data that is above the stability boundary.

On the CDF graph, the intersection points represent the values of logit probability which defines the separation line. On either side of the separation line, the proportion of incompatible points have the same proportion. The logit values show on the CDF graph the percentage of lying points that are below or above the separation line, on the stability graph. In Fig. 6, the logit value for stable-failure was determined as 0.91, and the value of the failure-major failure intersection equals 0.79. The intersection points on the graph define the optimum position of boundary for each stability class. From Fig. 6, it can be seen that the logit value for the stable-failure boundary is 0.92, and for failure-major failure, it equals 0.77. From the CDF graphs of each stability chart, it can be seen that the percentage of stable points that lies below the intersection point is equal to 24% and the same percentage of failure points lies above the intersection point.

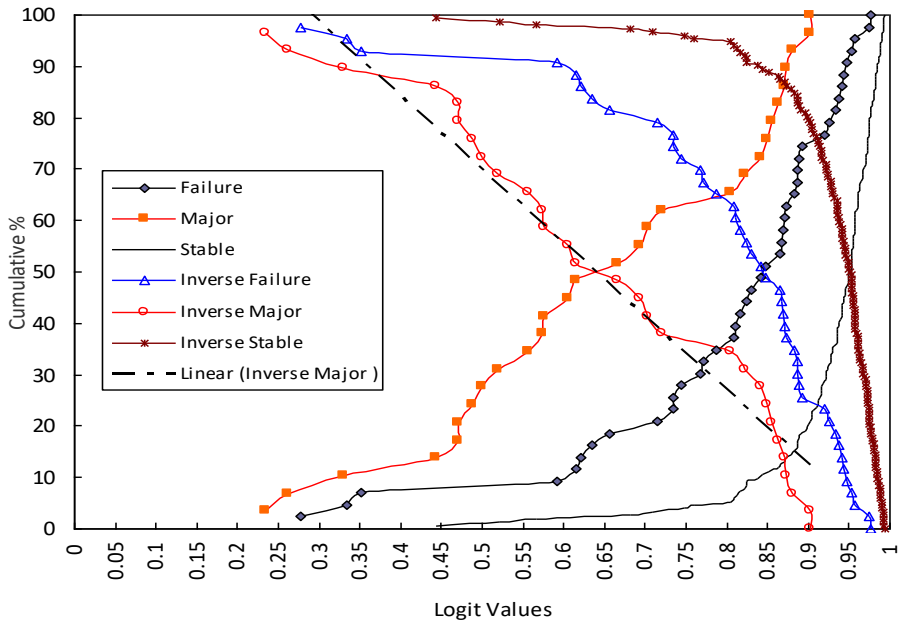

Fig 5 The CDF graph of Consolidated stability graph

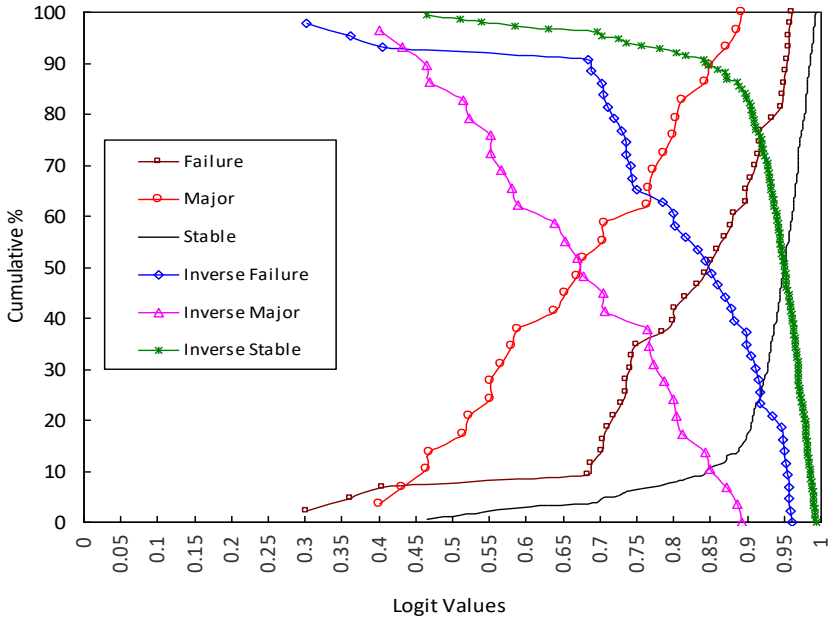

Fig 6 The CDF graph of Extended Stability graph

For the Consolidated stability graph, the log value obtained from Fig. 6 for the stable-failure intersection is equal to 0.92, and for failure-major failure, the intersection is determined as 0.79. Looking at Fig. 5, the intersection logit value of 0.92 shows a 24% discrepancy between stable and failure zones, which signifies that 24% of the failure logit values lie above the boundary while 24% of the stable logit values are located below the boundary. In the Extended Mathews stability graph, the intersection of the stable–failure curve equals 0.93, and for failure-major failure, the intersection is equal to 0.73 as can be seen in Fig. 6. In this case, also the discrepancy value equals 24 % and identical to that of the CDF of the Consolidated chart. For the stable-failure boundary of the Consolidated plot, the intersection logit value is 0.91 and the value of Z (the predicted log value) can be calculated as below:

$$Z = ln\left(\frac{0.91}{1-0.91}\right) = 2.31 \qquad (9)$$

The stable-failure boundary is calculated using Equation (8) and it becomes:

$$N = e^{\frac{(2.31-3.15-1.17lnS)}{0.84}} \Rightarrow N = e^{-0.82+1.62lnS} \qquad (10)$$

Similarly, for failure-major failure boundary, Equation (7) was used to determine Z as below:

$$Z = ln\left(\frac{0.79}{1-0.79}\right) = 1.325 \qquad (11)$$

Accordingly, the mathematical equation for failure-major failure boundary line becomes:

$$N = e^{\frac{(1.325-3.15-1.17lnS)}{0.84}} \Rightarrow N = e^{-2.07+1.62lnS} \qquad (12)$$

For the Extended stability graph, the intersection logit value of stable-failure boundary equals to 0.92 and Z becomes:

$$Z = ln\left(\frac{0.92}{1-0.92}\right) = 2.44 \qquad (13)$$

The boundary of stable-failure is defined by the following mathematical expression:

$$N = e^{\frac{(2.44-3.15-1.17lnS)}{0.84}} \Rightarrow N = e^{-0.65+1.62lnS} \qquad (14)$$

Similarly, in the Extended stability graph, the intersection logit value of stable-failure boundary equals to 0.76, and Z becomes:

$$Z = ln\left(\frac{0.77}{1-0.77}\right) = 1 \qquad (15)$$

The mathematical equation for failure-major failure boundary line becomes:

$$N = e^{\frac{(1-3.15-1.17lnS)}{0.84}} \Rightarrow N = e^{-2.48+1.62lnS} \qquad (16)$$

To find the probability function for stability classes (stable, failure, major failure) the gradient of CDF was used as illustrated in Figs. 7 and 8. The next step was to normalize the sum of these to 100, to determine the proportions of stability classes for a denoted logit value. To determine the position of stability boundaries, the intersection logit value was used which is based on incompatible points that are situated below and above the line, and the proportion of points are equal.

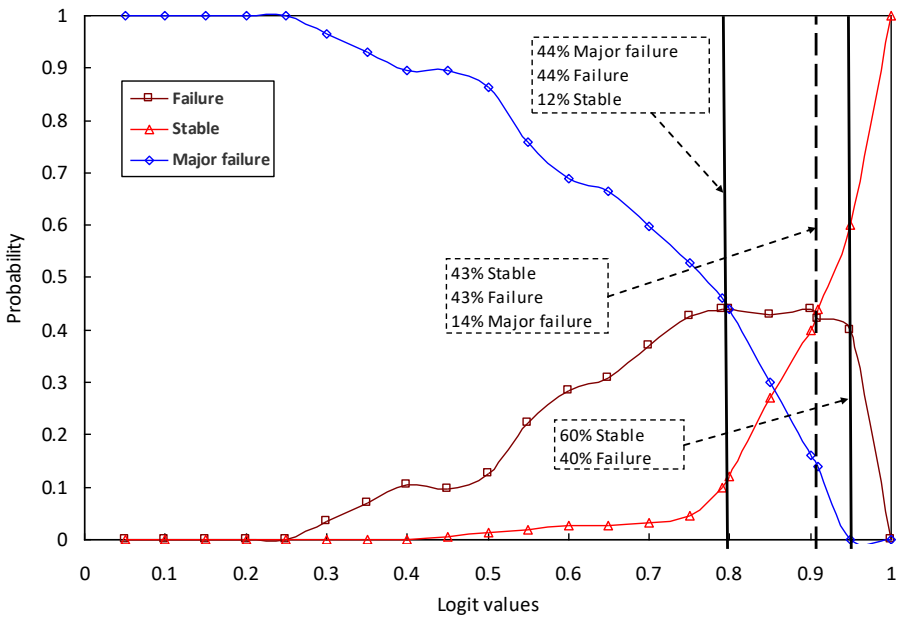

Fig 7 Consolidated graph probability density functions of stability data obtained from the logit probability values

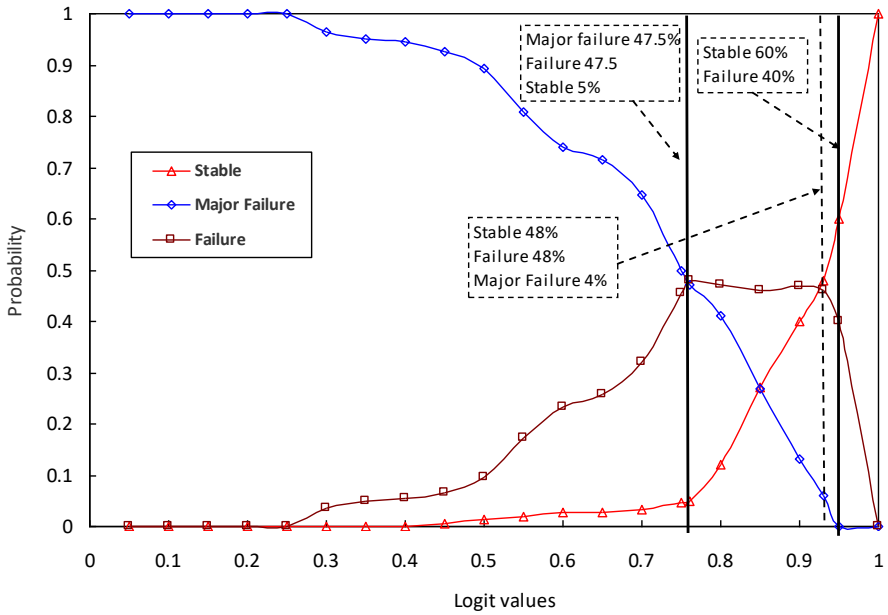

Fig 8 Extended graph probability density functions of stability data determined from the logit probability values

Using probability functions illustrated in Figs. 7 and 8, the values of estimated stability outcomes can be obtained for each stability class. To find the location of stability boundaries, the intersection points that were obtained from Figs. 5 and 6 are used, and the total sum of each class of stability for the defined intersection points is equal to 1.

From the probability function, it can be seen that when delineating the boundary of the stable-failure boundary statistically, it is the same for both graphs. In the case of failure-major failure boundary, due to the scarce number of cases, the boundary is not the same. The stability-failure boundary proportion for the Consolidated graph is 60% stable and 40% of failure. For the failure-major failure zone, the boundary proportion was identified as failure 45%, major failure 45%, and stable 10%, and the stability chart was constructed (Fig. 9).

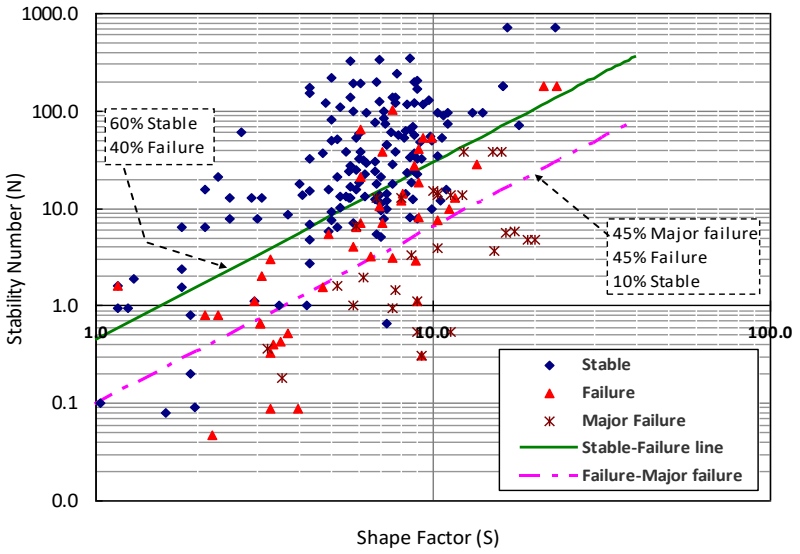

Fig 9 Consolidated stability graph for non-entry methods

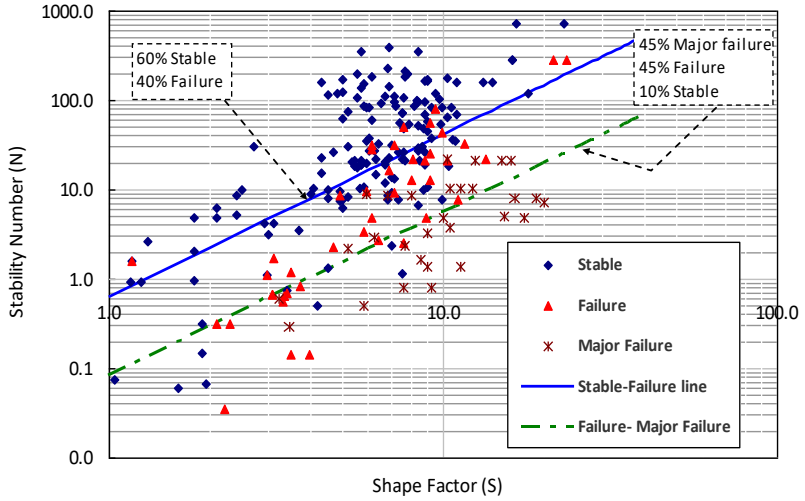

Fig 10 Extended stability graph (Non-entry mining methods data eliminated)

3.4. Model verification

The application of the logit model is related to the binary outcomes (yes/no), and in this research the dependent variables (classes of stability), three discontinuous categories are used in comparison with the typical logit model. Therefore, the logit model for this particular work is investigated due to the reason that it has three outcomes compared to the traditional model. The three-level logit model was denoted as a modified logit model to distinguish it from the traditional logit model. The stability outcome (Z) is a dependent variable in the model and relates to the stability data. For each class of stability (stable, failure, major-failure) the stability outcome is assigned, which has a numerical value. In the traditional binary logit model, the outcomes for the dependent value are either one or zero. Using the same principle all stable points were assigned as one (Z=1), and the remaining points (failure) were rated

as zero (Z=0). Then the CDF graph was constructed to determine the intersection logit value of stable and inverse failure curves. To delineate stability boundary, Equations (7) and (8) are used as below:

$$Z = ln\left(\frac{0.89}{1-0.89}\right) = 2.09 \qquad (17)$$

$$N = e^{\frac{(2.09-3.146-1.17lnS)}{0.84}} \Rightarrow N = e^{-1.1+1.62lnS} \qquad (18)$$

The same method was used for the major-failure logit model, the failure points were defined as one (Z=1), while for the major-failure stability outcome becomes a zero (Z=0) (see Equations 7 and 8).

$$Z = ln\left(\frac{0.78}{1-0.78}\right) = 1.27 \qquad (19)$$

$$N = e^{\frac{(1.27-3.15-1.17lnS)}{0.84}} \Rightarrow N = e^{-2.14+1.62lnS} \qquad (20)$$

In the traditional binary logit model, the outcomes are either stable or failure and major-failure or failure. For the three-logit model, two intermediate categories were used. The computed separation lines of the binary- and three-logit model are compared against one another in Fig. 11. The determined boundary lines have similar orientations and trends but differ in the location on the stability chart.

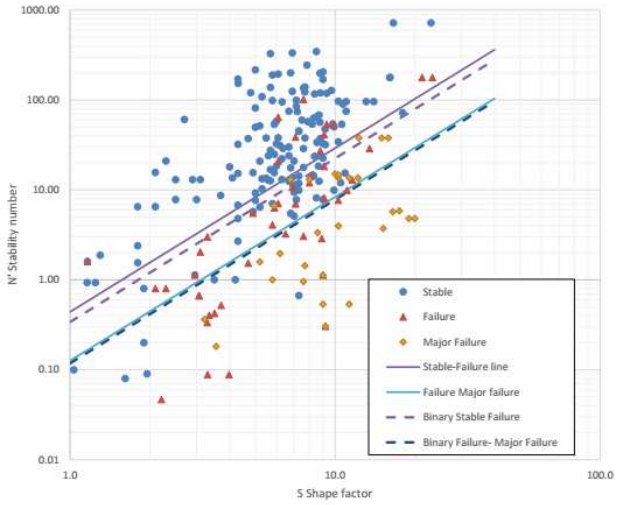

Fig 11 Comparison of stability boundaries obtained from binary- and three-logit models on the Consolidated Stability graph

To further verify the developed model, an open stope case study (Mawdesley 2002) was used employing the new Consolidated stability chart. In this example, five different geometric surfaces were examined. The shape factor was calculated from the geometry of the stope and shown in Table 5.

Table 5 Stope geometry data

Stope Surface	Height (m)	Length (m)	Area (m^2)	Perimeter (m)	Shape factor (S)
North End wall	46	15	690	122	5.7
South End wall	46	15	690	122	5.7
Footwall	46	28	1288	148	8.7
Hanging wall	46	28	1288	148	8.7
Crown	15	28	420	86	4.9

To calculate the modified stability number (N'), it was assumed that the joint water reduction and stress reduction factors are equal to one and Q' values were determined as below. The Q' value is determined by instructions outlined by the NGI Q classification system (Barton et al, 1974).

$$Q' = \frac{RQD}{Jn} \times \frac{Jr}{Ja} \qquad (21)$$

Where,

Q': The modified Q value,
RQD: Rock Quality Designation,
J_n: Joint set number,
J_a: Joint alteration number,
J_r: Joint roughness number

The calculated Q' values for the five stope surface geometries are presented in Table 6. To find the modified stability number (N'), Equation (1) was used and the values of adjustment factors A, B, and, C were determined. The values of the modified stability number (N') are given in Table 7.

Table 6 Rock mass quality data

Stope Surface	RQD	J_n	J_r	J_a	Q' value	Description
North End wall	58	7	2	1	16.6	Good
South End wall	66	5	2	1	26.4	Good
Footwall	66	6	3	1	33	Good
Hanging wall	80	15	1.5	4	2	Poor
Crown	79	13	2	2	6.1	Fair

Table 7 The calculated stability number for each stope surface

Surface	Q'	A	B	C	N'
North End wall	16.6	0.24	0.2	8	6.4
South End wall	26.4	0.24	0.2	8	10.2
Footwall	33	0.54	0.5	6.7	59.7
Hanging wall	2	0.54	0.5	6.7	3.62
Crown	6.1	0.15	0.8	2	1.44

After the calculation of shape factor and stability number, each stope surface was plotted on the Consolidated stability graph and the stability zone for each surface was determined. Then, the determined stability number and shape factor were substituted into Equation (6) and the logit value for each of the stope surfaces was calculated. Accordingly, the predicted logit values were substituted into Equation (7) and the predicted logit probability value for each surface was determined. The calculated results are presented in Table 8 and shown in Fig. 13. The determined logit probability values for each excavation surface was used to determine the probability of stability state of each surface from the probability functions as illustrated in Fig. 12.

Table 8 The predicted log values and logit probability values for all stope surfaces

Surface	Predicted log values (Z)	Logit probability value (P)
North End wall	1.92	0.87
South End wall	2.3	0.91
Footwall	3.1	0.96
Hanging wall	0.86	0.7
Crown	0.96	0.73

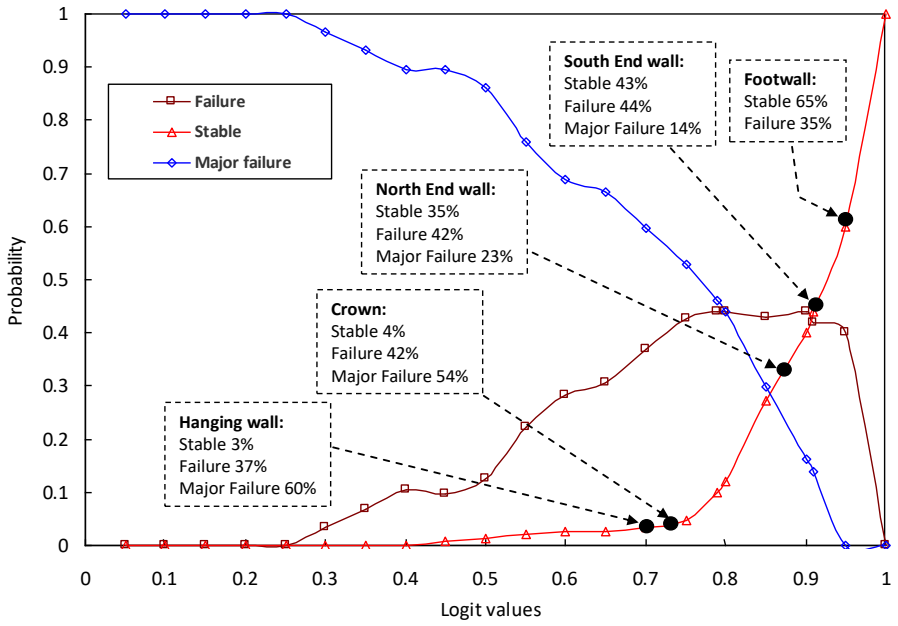

Fig 12 Plot of probability function for each stope surface determined from the logit model

Looking at the computed probability function charts, the state of various stope surfaces can be determined. The state of the stope surfaces of the analyzed case study is plotted on the Consolidated stability chart and illustrated in Fig. 13. For this example, the back and hanging wall of the stope lie below the failure-major failure envelope and plot within the caved zone. The South end wall and footwall state fall within the stable zone, and the north end wall state plot within the stable-failure zone.

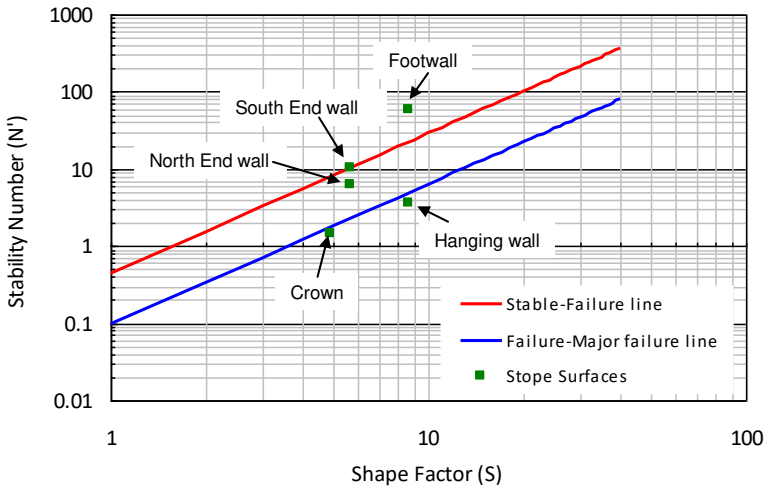

Fig 13 The stability state of the stope surfaces using the Consolidated stability graph

4. Discussions and Conclusions

The original stability graph by Mathews (1981), has been significantly modified in the past two decades and there are two commonly used modified graphs. The Extended stability chart, which is based on the original stability number and some adjustment factors, and the Modified stability graph, which is based on the modified stability number proposed by Potvin (1989). Looking at the relevant published literature on the subject, there have been differences of opinion among authors and this has led to confusion on the applicability of this empirical design method within the mining industry. The original version of the stability graph was developed for the design of the open stope mining methods, and since then, the database was extended and included entry mining methods leading to data heterogeneity in the database. The objective of this study was to remove all entry mining methods data from the extended database and produce a new graph based on the modified stability number (N').

The logistic regression was used as the fundamental tool for delineating the boundaries. The advantage of logistic regression is its ability in determining the probability functions of each stability class, which in turn enables one to determine the probability of instability and associated risks. Employing logistic regression enabled a more optimal and accurate placement of boundary zones. The advantage of this method is the usage of maximum likelihood estimates to minimize uncertainties. To investigate the accuracy of the model, the obtained logit probability values were compared with the initial data of the stability values. To reproduce the three classes of stability (stable, failure, major-failure), the stability data of the Mathews was investigated by implementing a three-level logit model. The development of a three-level logit model was substantiated. The location of each boundary was determined separately by a binary model and then the results were compared with the three-level model.

To demonstrate the applicability of the proposed Consolidated stability chart, an open stope example was illustrated. A typically inclined stope was considered and the stability state of five stope surfaces was analyzed. The probability of each stope surface stability was calculated using the logistic regression model and the developed Consolidated stability chart. The calculated shape factor and stability number for each stope surface were substituted into the logit equation and the probability of stability for each stope surface was determined. The stability of the footwall and south end wall is acceptable based on the Consolidated stability chart. This should be verified against on-site observations. The hanging wall and crown area are unstable the adapted stope design for this geometry must be revised. Alternative mining sequences or support measures can be used to avoid failure and dilution. The situation in the north wall is also of concern and this wall is potentially unstable. To assure safe operation, similar remedial measures, as for hanging wall and crown, should be adapted. The above stope example stability was analyzed by (Mawdesley 2002) using the Mathews Extended stability chart and data. Using the Extended stability chart, the stope footwall, south end wall, and north end wall plot well within the stable zone and above the stable-failure envelope. The hanging wall and crown areas of the stope lie within the stable and failure boundaries. Accordingly, the developed Consolidated chart, in which the entry-method data is excluded, produces a more conservative and safer design.

Once the probability of stability is known, one can determine the level of risk associated with each stope surface with regard to field observations of failure mode and extent. Knowing and defining the consequences of instability, a case-specific cost-risk relationship must be developed. Accordingly, preventive measures can be taken to avoid failure and fall of ground associated risks. It should be realized that the suggested solutions will minimize the impact of instability and failure. More rigorous stability analyses are required to investigate the failure mechanisms and revise the design as appropriate. As outlined by many practitioners, a major limitation of the Mathews method is its site-specificity. The application of logistic regression enabled the quantification of this site-specificity. Furthermore,

logistic regression was used to determine stability boundaries. The newly developed stability graph can be used as a design tool for non-entry mining methods with more confidence. The developed Consolidated stability graph is still a work in progress and more efforts are required to increase the reliability of the new graph. It can be improved by incorporating new adjustment factors such as stand-up time, fault-factor, and blasting effects. Furthermore, adding the relevant field and observational data to the database will enhance its accuracy and reliability.

5. Declarations

The authors declare that they have no conflict of interest and this study was not funded by any organization.

6. References

Barton N (1976) Recent experiences with the Q-system of tunnel support design. *Proceedings of the Symposium on Exploration for Rock Engineering*. November 1976:107-117

Bieniawski ZT (1973) Engineering classification of jointed rock masses. Civil Engineer in South Africa, 15 (12):335-343

Clark L, Pakalnis R (1997) An empirical design approach for estimating unplanned dilution from open stope hanging walls and footwalls. In Proceedings of the 99th annual general meeting. Vancouver: Canadian Institute of Mining, Metallurgy and Petroleum

Hoek E, Kaiser PK, Bawden WF (1995) Support of underground excavations in Hard Rock. Rotterdam, Balkema:215p

Laubscher DH, Taylor HW (1976) The importance of geomechanics classification of jointed rock masses in mining operations. Proceedings of the Symposium on Exploration for Rock Engineering, Johannesburg, South Africa

Liao TF (1994) Interpreting Probability Models: Logit, probit, and other generalized linear models. Sage University Paper series on Quantitative Applications in the Social Sciences. California; Sage:88p

Mathews KE, Hoek E, Wyllie DC, Stewart SBV (1981) Prediction of stable excavation spans at depths below 1000m in hard rock mines. CANMET Report, DSS Serial No. OSQ80-00081

Mawdesley C, Trueman R, Whiten WJ (2001) Extending the Mathews stability graph for open–stope design. Mining Technology, 110(1):27-39

Mawdesley C (2002) Predicting rock mass cavability in block caving mines. Dissertation, The University of Queensland

Milne DM, Pakalnis RC, Lunder P J (1996) Approach to the quantification of hanging-wall behaviour. Trans Inst Min Metall, Sect A: Min Industry, 105:A64-69

Milne D, Pakalnis R, Grant D, Sharma J (2004) Interpreting hanging wall deformation in mines. International Journal of Rock Mechanics and Mining Sciences, 41(7):1139-1151

Nickson SD (1992) Cable support guidelines for underground hard rock mine operations. Ph.D. Dissertation, University of British Columbia

Potvin Y (1988) Empirical open stope design in Canada. Ph.D. Dissertation, University of British Columbia

Potvin Y, Hadjigeorgiou J (2001) The stability graph method. Underground Mining Methods:513-520

Suorineni FT (1998) Effects of faults and stress on open stope design. Ph.D. Dissertation, University of Waterloo

Suorineni FT, Henning JG, Kaiser PK (2001) Narrow-vein mining experiences at Ashanti: Case study. International National Symposium, Mining techniques of Narrow-vein Deposits. Val'Dor, QC: Canadian Institute of Mining, Metallurgy and Petroleum

Stewart SBV, Forsyth WW (1995) The Mathew's method for open stope design. CIM Bulletin, 88(992):45-53

Stewart PC, Trueman R (2001) The Extended Mathews Stability Graph: Quantifying case history requirements and site-specific effects. In International Symposium on Mining Techniques:84-92

Stewart PC (2005) Minimizing dilution in narrow vein mines. PhD Dissertation, Julius Kruttschnitt Mineral Research Centre, The University of Queensland

Trueman R, Mikula P, Mawdesley CA, Harries N (2000) Experience in Australia with the application of the Mathew's method for open stope design. The CIM Bulletin, 93(1036):162-167

Trueman R, Mawdesley C (2003) Predicting cave initiation and propagation. CIM bulletin, 96(1071):54-59

Vallejos JA, Delonca A, Perez E (2018) Three-dimensional effect of stresses in open stope mine design. International Journal of Mining, Reclamation and Environment. 32(5):355-374